Superconducting transition, fluctuation, and vortex motion in a two-dimensional single-crystal Nb film

J. W. P. Hsu* and A. Kapitulnik
Department of Applied Physics, Stanford University, Stanford, California 94305
(Received 30 July 1991; revised manuscript received 25 September 1991)

We report a detailed study on the transport properties of an ultrathin single-crystal Nb film, whose thickness ($d \approx 20$ Å) is less than all other relevant length scales except the lattice constant. The two-dimensional (2D) nature of the sample in the superconducting state is reflected in the characteristic distinction between its parallel and perpendicular critical fields, as well as in the temperature dependence of the fluctuation conductivity. Because of the long mean free path of this single-crystal film, we find it necessary to include both Maki-Thompson and Aslamazov-Larkin terms in the fluctuation-conductivity analysis. The logarithmic temperature dependence of the resistance, signature of the 2D electron-electron interaction effect, has been observed when the external magnetic fields exceed the upper critical field, indicating that the sample is also two dimensional in its normal state. In addition, dissipation below T_c under small applied current is attributed to vortex motion; activation energy as a function of magnetic field has been obtained via the application of the Anderson-Kim model extended to two dimensions. The characteristics of the Kosterlitz-Thouless transition, which has been observed only in high-resistance 2D superconducting films, have been seen in our relatively low-resistance Nb film, although they are greatly affected by the presence of strong pinning. This work provides insight into the non-equilibrium properties of clean 2D superconducting films.

I. INTRODUCTION

The physics of two-dimensional (2D) metals and superconductors has been an interest of research for the past 20 years. Although not every question has been answered, numerous breakthroughs in theory and experiment have greatly improved the understanding of 2D systems. This paper is concerned with the electric transport properties of an ultrathin epitaxially grown 20-Å niobium (Nb) film. Transmission-electron-microscopy (TEM) studies indicated that these films were single crystals. Because of the thickness being much shorter than the bulk coherence length ($\xi^{\text{bulk}} = 395$ Å) and penetration depth ($\lambda^{\text{bulk}} = 345$ Å),[1] these samples are 2D. This system is both interesting and unique because of the small amount of disorder. Experiments on 2D superconductors have so far been performed on materials with electron mean free paths limited by disorder, e.g., polycrystalline or granular Al (Refs. 2 and 3) and amorphous MoGe films.[4] On the other hand, the mean free path of our single-crystal Nb is limited by the film thickness and not by disorder. Park[5] demonstrated that high-quality tunnel junctions on similar Nb films as thin as 16 Å can be produced with a high success rate. The thinner films ($d_{\text{Nb}} \leq 50$ Å) displayed an enhancement of the gap-to-T_c ratio from the Bardeen-Cooper-Schrieffer (BCS) weak-coupling value $2\Delta/kT_c = 3.52$ to as large as 5.2 for a 9-Å film.[5] In this paper we investigate other transport properties. Although some results are typical of 2D superconductors, interesting results on the superconducting transition and vortex motion in clean 2D films have also been found.

The paper is organized as follows: In the second section we discuss experimental details emphasizing the quality of the samples and characterization methods. The third section is devoted to experimental results and discussion of fluctuation conductivity. The fourth section is used to show the relevance of the Kosterlitz-Thouless theory to the superconducting transition and the effect of small magnetic fields on the resistive tails. The fifth section contains a detailed study of the resistive tails in perpendicular magnetic fields; results are analyzed within the framework of vortex motion. Current-voltage (I-V) characteristics near the superconducting transition temperature (T_c) are also included here. Part of this section has been previously published as a letter.[6] In the sixth section, we present high-field results, concerning the destruction of superconductivity by magnetic fields and transport properties of this system in the normal state. A summary is presented in the last section.

II. EXPERIMENTAL DETAILS

A. Sample preparation and characterization

All samples were made by electron-beam evaporation onto ($\frac{1}{4}$-in.)^2 polished single-crystal R-plane ($1\bar{1}02$) sapphire substrates. After acid and solvent cleaning, the substrates were outgassed at 750 °C for 1 h in the deposition chamber after the evaporator had been baked out overnight. During the substrate outgassing, the sources were also outgassed for ≈ 10 min to remove the surface oxide. The usual base pressure in the evaporation chamber was in the low 10^{-8} Torr. The substrates were then cooled down to the deposition temperature (≈ 100 °C), chosen to be high enough to produce good quality ultrathin Nb films, but not so high that diffusion between the overlayer amorphous Si (α-Si) and the bottom Nb layer would be significant.

To produce high-quality films consistently, the substrates were cleaned with a 500-eV Ar^+-ion beam for ≈ 1 min prior to Nb deposition. This step is crucial. After bringing the Nb sources up to a rate of ≈ 5 Å/sec, ≈ 20 Å of Nb was deposited. The Nb thickness was controlled by the time the main shutter was opened, using rates calibrated from the evaporation time of thicker films. Immediately, after the deposition of Nb, ≈ 30 Å of α-Si was deposited to protect the Nb from oxidation. The times between ion-beam cleaning, deposition of the Nb layer, and deposition of the α-Si layer were minimized (≈ 1 min each case) in order to reduce oxide formation at the interfaces.

The crystallinity of the Nb films was investigated with TEM. The sample (with Nb and Si already deposited) were thinned down to ≈ 250 μm from the substrate side, and $a \approx 5$-mm-diam hole was cut. At the edge of the hole, the sample was thin enough (≈ 1 μm) for TEM. The beam aperture was 1–5 μm, and several pictures at different places were taken. Energy dispersive x-ray (EDX) spectroscopy was also employed to check the elements in the samples.

Figure 1 shows typical TEM diffraction patterns of two samples made in the same runs as $A1$ and $A4$. $A2$ [Fig. 1(a)] was ion-beam cleaned, while $A3$ [Fig. 1(b)] was not. The diffraction spots, instead of rings, suggest that the Nb layer is single crystal. In Fig. 1(b) one can clearly see that the Nb and Al_2O_3 diffraction spots mismatch in one direction, but match in the other. However, the ion-beam-cleaned sample (A2) shows perfect lattice match between the Nb and sapphire. The Nb grows on the R-plane sapphire in the [100] direction, where the relevant Nb lattice spacing is that of the (110) planes (2.33 Å), and the relevant Al_2O_3 spacings are the (104) planes (2.55 Å) and (110) and (2.39 Å). Although the lattice mismatches between Nb and Al_2O_3 are quite significant (9.4% and 2.6%), one can see that epitaxial growth can be achieved when ion-beam cleaning precedes Nb deposition. Figure 1(a) shows a diamond, instead of a cubic, structure, reflecting spacings of the sapphire substrates and not of the Nb. Tunneling results also showed that ion-beam-cleaned samples were far superior,[5] for more details of the role of ion-beam cleaning in this system, see Ref. 7.

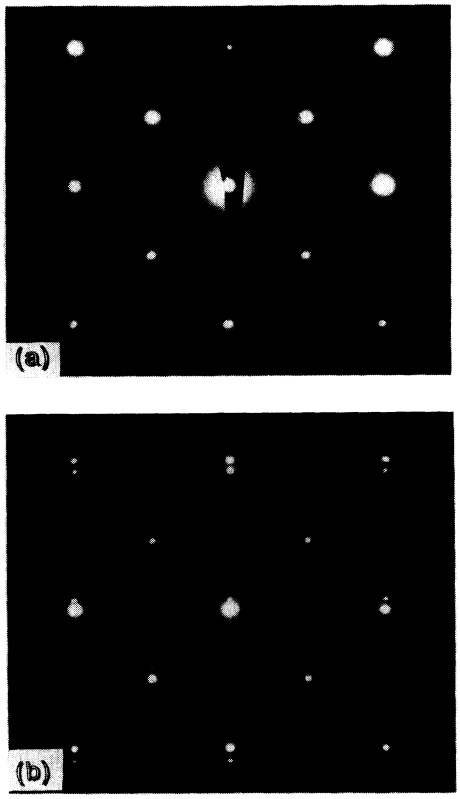

FIG. 1. Typical TEM diffraction patterns of ultrathin Nb described in the text: (a) sample with ion-beam-cleaned substrate (A2) and (b) sample with uncleaned substrate (A3).

The samples were patterned by photolithography for four-point resistance measurements into a line of width (w) 96 μm, with the distance between voltage leads (L) $20w$ ($L \approx 1.9$ mm). Resistance as a function of temperature was measured down to ≈ 1.6 K, using both dc and ac lock-in methods. The measurement current was 1 μA, corresponding to a current density of 5.2×10^2 A/cm^2, assuming all of the current flows through the Nb and not through the α-Si. This current is in the Ohmic (linear) $I-V$ regime. The temperature was measured with a carbon-glass thermometer buried in the copper sample block. The relative temperatures between different runs, with the sample position fixed with respect to that of the thermometer, were accurate to ≈ 1 mK.

The zero-field measurements were performed in a Degaussed μ-metal-shielded Dewar. The exact field inside the shielded Dewar is unknown, but is estimated to be $\lesssim 30$ mG. In addition, magnetic fields up to 100 G were obtained in this Dewar using a copper coil. The 60 G to 8 kG measurements were performed in a rotatable electromagnet. To determine the field orientation perpendicular to the plane of the film, we first measured the resistance at fixed temperature and field near T_c as a function of angle near parallel orientation. When the resistance was a minimum , the field was parallel to the film surface. The magnet was the swung 90° for the perpendicular-field measurement. The alignment accuracy was about 0.1°, assuming the plane of the film was vertical. Because the resistance depends only weakly on angle when the field direction is near perpendicular, if the plane of the film was not exactly vertical, the results were not greatly affected. Using this alignment procedure, data on the upper critical field (H_{c2}) for parallel and perpendicular directions were taken. High-field measurements ($H = 1-8$ T) were done in a superconducting magnet with the sample mounted perpendicular to the field.

The single-crystal Nb film studied here has normal-state sheet resistance $R_\square = 122$ Ω/□ (corresponding to a resistivity $\rho_N \equiv R_\square d$ of 24 $\mu\Omega$ cm), mean free path $l \approx 35$ Å (see below), and mean field $T_c = 3.725$ K determined from fitting the fluctuation conductivity using both Aslamazov-Larkin and Maki-Thompson theories.[8] Fitting the temperature dependence of the zero-field resistive transition to the theory of Halperin and Nelson[9] yielded the Kosterlitz-Thouless (KT) transition temperature $T_{KT} = 3.60$ K (see Sec. IV). Figure 2 depicts the

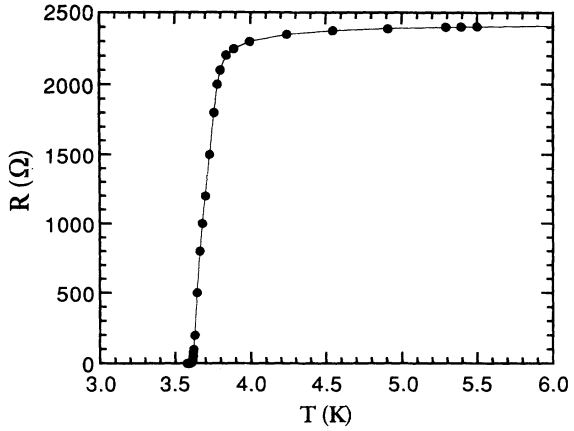

FIG. 2. R vs T of a 20-Å Nb film in zero applied field.

resistive transition in zero field. Because of the mean path being thickness limited,[5] e.g., $l \sim d$, the resistivity of these Nb films is greater than that of the bulk Nb.

B. Effect of parallel versus perpendicular applied fields

We show in this section the effect of parallel versus perpendicular fields on the superconducting transition. Because resistance is a strong function of the angle between the field direction and film plane when they are nearly parallel, a careful alignment procedure is critical, as described above. "Parallel" is defined as the angle where resistance is minimum.

Figure 3 shows H_{c2} as a function of temperature (actually T_c as a function of H) for both parallel and perpendicular fields. T_c here is defined as the temperature at which $R=0.5R_n$. While a small perpendicular field suppresses T_c significantly ($dH_{c2}^{\perp}/dT_c \approx 7$ kG/K), parallel fields no not show any effect on T_c until 5 kG, as expected for thin films. In the Ginzburg-Landau (GL) theory, for films thinner than the perturbation depth (λ), the critical field, in the parallel direction,

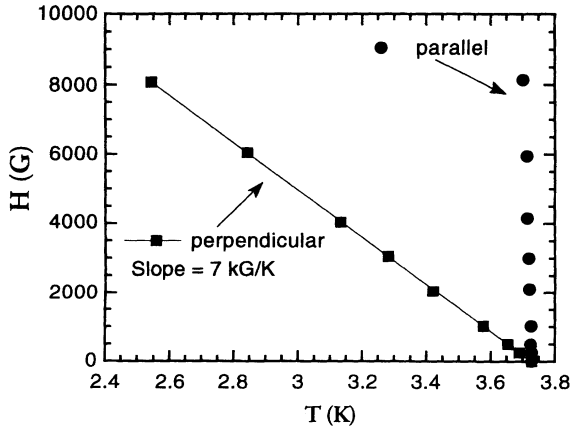

FIG. 3. H_{c2} vs T for both parallel and perpendicular fields.

$$H_c^{\parallel}=2\sqrt{6}\left[\frac{H_c\lambda}{d}\right]=\frac{\sqrt{3}\Phi_0}{\pi\xi(T)d}\propto\sqrt{1-T/T_c}\ . \tag{1}$$

whose slope ($dH_c^{\parallel}/dT_c|_{T_c}$). This can be seen in Fig. 3.

Recently, Kogan calculated T_c as a function of parallel fields, taking into account the field dependence of the coherence length.[10] He found that for sufficiently thin and clean films, a T_c enhancement in small parallel fields occurs. Although according to his results our Nb film satisfies the criterion for observing this T_c enhancement, we saw no hint of such non-GL behavior.

C. Determination of sample parameters

We derive the various parameters which are relevant to the analysis in this paper, as well as verify the 2D nature of our sample. In the dirty limit,[11]

$$\xi(t)=\frac{\xi(0)}{\sqrt{1-t}}$$

and

$$\lambda(t)=\frac{\lambda(0)}{\sqrt{1-t}}\ ,$$

where $T=T/T_c$, $\xi(0)=0.855\sqrt{\xi_0 l}$, $\lambda(0)=\lambda_L(0)\sqrt{\xi_0/2.66l}$, ξ_0 is the BCS coherence length, and $\lambda_L(0)$ is the London penetration depth at $T=0$. We emphasize that $\xi(0)$ and $\lambda(0)$ are not the zero-temperature values of coherence length and penetration depth; they are merely the coefficients of the temperature-dependent $\xi(T)$ and $\lambda(T)$ for $T \lesssim T_c$. The factor of 2.66 in $\lambda(0)$ comes from twice the kernel, $J(0,T)=1.33$ at $T=T_c$. (See Ref. 11, pp. 67–68.) Note that all values obtained here are valid only in the GL region, $T \approx T_c$.

Only three experimentally measured values are needed to extract the various superconducting parameters: $-dH_{c2}/dT|_{T_c}$, ρ_n and T_c. Because of the field dependence of the transition width, the determination of H_{c2} and T_c is ambiguous, as in the case of high-T_c cuprates. In our sample, T_c at $T=0.5R_n$ is least complicated by the resistive tails (which could be due to flux creep or KT vortex pairs unbinding) and is reduced linearly as H is increased, which is the expected in pair-breaking theory.[12] Hence we use the valences of $-dH_{c2}/dT|_{T_c}$ at $0.5R_n=7$ kG/K (see Fig. 3) and $T_c=3.725$ K (determined from fluctuation conductivity) to obtain other superconducting parameters. We find $\kappa \simeq 14.5$, $\xi(0) \simeq 104$ Å, and $\lambda(0) \simeq 1600$ Å. The perpendicular penetration depth is

$$\lambda_{\perp}(t)\equiv\frac{\lambda^2(t)}{d}=\frac{\lambda_{\perp}(0)}{1-t}\ , \tag{2}$$

with $\lambda_{\perp}(0) \simeq 12.8$ μm, smaller than the sample width w.

We can estimate $H_{c2}(0)$ using pair-breaking theory, which extends the validity of GL theory to $T=0$:[12]

$$H_{c2}(0)=0.825\left[-\left.\frac{dH_{c2}}{dT}\right|_{T_c}\right]T_c \ . \tag{3}$$

The numerical factor is proportional to $2\Delta/kT_c$; for BCS weak-coupling superconductors with $2\Delta/kT_c=3.52$, it equals 0.69. Since the $2\Delta/kT_c=4.2$ for our sample, the prefactor is larger. The $H_{c2}(0)$ estimated from Eq. (3) is 2.15 T. In this model, $-dH_{c2}/dT|_{T_c}$ is related to the pair-breaking strength, which is related to the diffusion constant D for our sample:

$$D=1.52\frac{ck}{e\,dH_{c2}/dT|_{T_c}}\approx 1.8\ \text{cm}^2/\text{sec} \ . \tag{4}$$

Using $\xi_0=395$ Å (Ref. 1) and $\xi(0)=0.855\sqrt{\xi_0 l}=104$ Å, we estimate the mean free path, $l\simeq 38$ Å. While from the Einstein relation $\sigma_n=1/\rho_n=e^2D\nu(0)$, where $D=\frac{1}{3}v_F l$ and $\nu(0)$ is the density of states at the Fermi energy, we obtain $l\simeq 32$ Å using the Fermi velocity $v_F=2.7\times10^7$ cm^2/sec and $\hbar v_F(0)=1.65\times10^{15}$ cm^{-2}.[13] The mean free paths obtained from the two methods are in excellent agreement, with $D\simeq 3.2$ cm^2/sec slightly larger than D obtained from Eq. (4), which corresponds to $l=20$ Å, the thickness of the film. It is possible that scattering at the Nb/α-Si interface produces a pair-breaking mechanism not reflected in the elastic mean free path determined from the normal-state resistance. Of course, this small discrepancy could simply be caused by the ambiguity of $dH_{c2}/dT|_{T_c}$ because of the field broadening of the transition width.

III. FLUCTUATION CONDUCTIVITY

A. Theoretical considerations

The presence of superconducting fluctuations above T_c causes excess conductivity $[\sigma'(T)\equiv\sigma(T)-\sigma_n]$, which is enhanced in reduced dimensions (2D and 1D) as compared to bulk (3D) samples. 2D is an especially interesting case because the theoretically predicted excess *conductance* is a universal function of the reduced temperature,

$$\tau\equiv\frac{T-T_c}{T_c} \ ,$$

independent of material parameters, such as the coherence length present in the formulae for 3D and 1D.

There exist two contributions to the fluctuation conductivity: the direct Aslamov-Larkin (AL) term[14] and the indirect Mako-Thompson (MT) term.[15,16] The AL contribution results from the direct acceleration of the fluctuation-induced Cooper pairs above T_c; in 2D,

$$\sigma'_{\rm AL}=\frac{e^2}{16\hbar d}\frac{1}{\tau} \ , \tag{5}$$

where d is the sample thickness. As pointed out above, the fluctuation conductance $G'_\square\equiv\sigma'_{\rm Al}d$ is independent of $\xi_{\rm GL}$. Experiments on amorphous Bi, Ga, and Pb films have confirmed both the temperature dependence and universality of $G'_\square$.[17]

However, a larger σ' than predicted in Eq. (5) was observed in the case of clean Al films (small $R_\square$).[18] To explain this, one must include the MT term, which has an anomalous temperature dependence,

$$\sigma'_{\rm MT}=\frac{e^2}{8\hbar d}\frac{1}{\tau-\delta}\ln\left[\frac{\tau}{\delta}\right] \ , \tag{6}$$

where δ is a "pair-breaking parameter" discussed below. This term originates from the inertia of the superconducting pairs after decaying into pairs of quasiparticles with opposite momenta. Since elastic scattering by impurity potentials conserves time-reversal symmetry, these quasiparticle pairs continue to have nearly zero total momentum and to produce excess conductivity. The quasiparticle-pair lifetime (τ_ϕ) is limited by inelastic scattering, the presence of pair-breaking mechanisms (e.g., magnetic impurities, external fields), or by the formation of subsequent superconducting fluctuations. Maki's[15] result diverges at all temperatures for both 2D and 1D because of small $\mathbf{k}$ contributions to the phase space. Thompson[16] then introduced a cutoff [δ in Eq. (6)] to regulate this long-wavelength (infrared) divergence. In pair-breaking theory,[12] this lifetime is related to δ by

$$\delta=\frac{\alpha}{\alpha_c(0)}=\frac{\xi^2(0)}{D\tau_\phi} \ , \tag{7}$$

where α and $\alpha_c(0)$ are pair-breaking strengths defined in Ref. 12. The difference between τ_ϕ defined here and the inelastic-scattering time ($\tau_{\rm in}$) determined from magnetoresistance will be discussed below. For $\delta\neq0$, the MT term does not contribute near T_c ($\tau=0$), but $\sigma'_{\rm MT}=2\sigma'_{\rm AL}$ at the temperature $\tau=\delta$ and diverges for $\tau\gg\delta$. Consequently, the larger δ is, the less important the MT contribution is when analyzing σ' near T_c. This is why only $\sigma'_{\rm AL}$ was needed to explain the results of amorphous Bi.

Although the MT term has helped explain the excess conductivity in clean 2D films, the origin and magnitude of δ are poorly understood theoretically. Experimentally, δ depends on the sample sheet resistance $R_\square$ as well as on temperature. Fitting σ' in a restricted temperature region, Crow, Bhatnager, and Mihalism[19] found a linear relation between the temperature-independent part of δ and $R_\square$:

$$\delta_0=(A+BR_\square)10^{-4} \ , \tag{8}$$

where A and B are material-dependent parameters determined empirically. Starting from a microscopic theory with impurity scattering, Patton reanalyzed the fluctuation conductivity, including both direct and indirect terms. His results are more complicated, but can be approximated by $\sigma'=\sigma'_{\rm AL}+\sigma'_{\rm MT}$, where the divergence of $\sigma'_{\rm MT}$ is naturally cut off by the temperature-dependent pair breaker $\delta_1\sim10^{-5}R_\square/\tau$, which diverges at T_c because of the increasing probability for an electron to meet another electron of opposite momentum and spin and condense into a superconducting fluctuation.[20] Contrary to the empirical result of Eq. (8), the $R_\square$ and temperature dependence of δ_1 is specified by Patton's theory. Utiliz-

ing this, Craven, Thomas, and Parks analyzed the combined data of many researchers for fixed $\tau=0.03$ and found that $\delta=\delta_0+10^{-5}R_\square/\tau$ described in Al films very well, while results on Sn implied that additional $R_\square$ dependence in δ_0 was needed, and the MT term was unnecessary for Pb films with $R_\square \gtrsim 1\ \Omega/\square$.[21]

Nevertheless, the temperature dependence of δ_1 predicted by Patton was not investigated until recently. By fitting magnetoresistance data on clean Al films (with $R_\square < 70\ \Omega/\square$), Gordon, Lobb, and Tinkham[22] found that $1/\tau_\phi$, and hence δ, diverged near T_c:

$$\delta(T)=\delta_0+\frac{\alpha R_\square}{\ln(1+\tau)}\ , \tag{9}$$

and $\alpha\approx 10^{-5}$ for $\tau\lesssim 0.5$. They also showed that using this temperature dependent δ [Eq. (9)] instead of a temperature-independent δ produces a better fit to their fluctuation-conductivity data. Other experimental evidence of δ diverging near T_c was found in MoGe films ($R_\square = 300 \rightarrow 500\ \Omega/\square$) for $\tau\lesssim 0.005$,[23] but no such divergence was observed in high-$R_\square$ In/InO_x films ($R_\square > 2$ k$\Omega/\square$),[24] possibly as a result of the large value of δ_0; i.e., τ_0 in the experimental temperature regime was never limited by subsequent superconducting fluctuations.

B. Experimental results and analysis

Figure 4 shows the normalized inverse σ' as a function of T in zero field for both experimental data and a theoretical model fitted to the data,

$$\frac{e^2}{16\hbar d\sigma'}=\left[\frac{1}{\tau}+\frac{2}{\tau-\delta}\ln\frac{\tau}{\delta}\right]^{-1}\ , \tag{10}$$

where $\sigma'=\sigma(T)-\sigma_n$ and $\sigma_n=1/R_n d$. Instead of extrapolating R as a function of $1/H$ to zero or using the resistance at some arbitrary temperature to define R_n, we used the resistance in a perpendicular field of 8 T as R_n. Actually, the choice of R_n is not crucial here because, in the normal state, the resistance varies by $<1\%$ from 2 to 20 K. The first term in Eq. (10) is due to the AL contribution and the second is the MT contribution. It is clear from Fig. 4 that our data cannot be fitted with the AL term alone, represented by the dotted line in Fig. 4. Assuming a temperature-independent δ, we could fit our data to Eq. (10) (solid line in Fig. 4) with $T_c=3.725$ K and $\delta=0.18$ up to $\tau=0.16$. Depending on the temperature range used in the fitting, a slightly different value of δ was obtained, hinting that δ must be temperature dependent. The fitted value of T_c is more robust, varying between 3.72 and 3.73 K, which is near $R=0.5R_n$. (See Fig. 2.) This value is used as the BCS T_c of the sample.

Since T_c is known and the AL term depends on T_c only, we subtract σ'_{AL} from σ' and then solve for δ as a function of temperature. [See Eq. (10).] Figure 5 depicts δ as a function of reduced temperature τ. Note that δ seems to diverge as temperature is lowered toward T_c, as predicted by Patton[20] and discussed above. Since this divergence was not seen in high-resistance In/InO_x films,[24] it would be interesting to see whether it correlates with $R_\square$. Let us define τ_x as the reduced temperature at which δ starts to diverge (indicated in Fig. 5). Figure 6 shows that τ_x decreases as $R_\square$ increases; that is, as $R_\square$ increases, one needs to be closer to T_c (smaller τ) to see a divergence of δ. This makes sense because the average value of δ is greater for larger $R_\square$ samples, and pair-breaking mechanisms other than the formation of superconducting fluctuations are the dominant factor in determining τ_ϕ until T is very close to T_c.

Above τ_x, δ increases roughly linearly as T (Fig. 5), indicating that the dominant temperature dependence of $1/\tau_\phi$ is due to 2D electron-electron scattering,[25] consistent with magnetoresistance studies on rf-sputtered Nb films, which show that the inelastic-scattering rate ($1/\tau_{in}$) at $T=5$–10 K is $\propto T$.[26,27] The value of $\delta\simeq 0.15$–0.2 near T_c is rather large when compared to granular Al films of

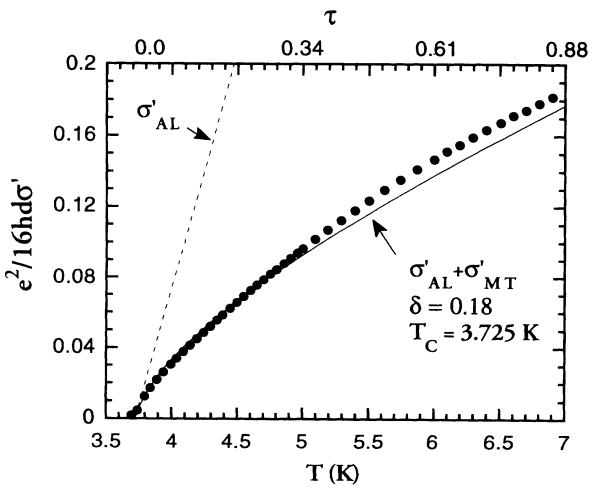

FIG. 4. Normalized inverse fluctuation conductivity vs temperature in zero field. The circles are experimental results. The dotted line indicates the contribution from the Aslamazov-Larkin term alone. The solid line is a fit to the data with temperature independent $\delta=0.18$.

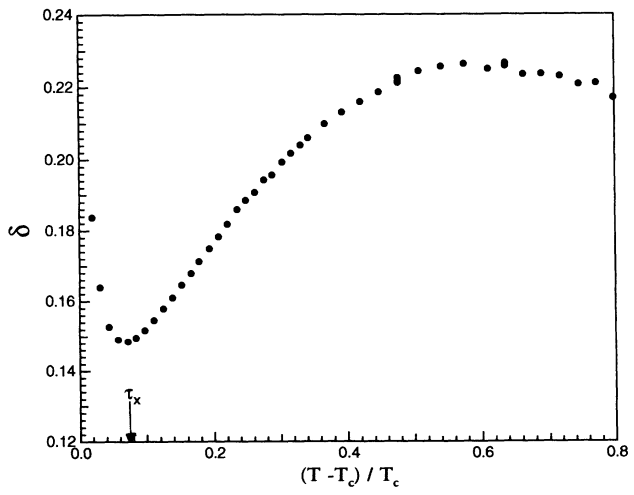

FIG. 5. δ vs reduced temperature.

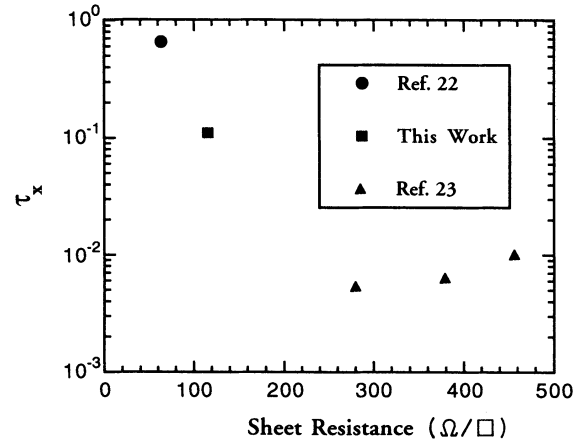

FIG. 6. τ_x (logarithmic) vs $R_\square$ for various materials: data taken from Ref. 22 (granular Al), Ref. 23 (amorphous MoGe), and this work (single-crystal Nb).

the same $R_\square = 122\ \Omega/\square$,[19]

$$\delta_{Al} \simeq 3\times10^{-4}+6\times10^{-4}R_\square \simeq 0.073\ ,$$

but is slightly less than the value for tin,

$$\delta_{Sn} \simeq 0.01+2\times10^{-3}R_\square \simeq 0.25\ .$$

Kawagut and Shibuya found that the MT term was not necessary to analyze fluctuation conductivity on quench-condensed Nb films; they obtained δ from 0.12 to 0.34 for film thicknesses 180 Å down to 70 Å.[28] Our result for δ is of the same order, but somewhat smaller. Since Ref. 28 used quench-condensed films, which are likely to be amorphous or polycrystalline with higher $R_\square$, it is not surprising that pair breaking is weaker in our single-crystal Nb film. However, the origin of this large pair-breaking effect in Nb films, as compared to Al, is not clear. Appel has proposed that the intrinsic pair breaking is caused by thermal phonons; thus the minimum value δ_{min} for a given material is proportional to $\lambda(T/\Theta_D)^2$, where λ is the electron-phonon coupling constant and Θ_D is the Debye temperature.[29] Since λ for Nb is ≈ 1.0, while $\lambda_{Al} \approx 0.4$,[30] and Θ_D for Nb is less than that for Al,[31] by this model, δ_{min} for Nb will be an order of magnitude larger than that for Al. This also holds when comparing experimental data on Nb and on Pb: Pb has a larger λ, a smaller Θ_D, and a larger measured δ.

Although our value of δ is comparable to those in the literature, a discrepancy occurs when we use Eq. (7) to convert δ to τ_ϕ. $\delta=0.18$ corresponds to $1/\tau_\phi = 1.66\times10^{12}\delta = 3\times10^{11}$ sec^{-1} (or $\tau_\phi = 3.3\times10^{-12}$ sec), which is a few times larger than the $1/\tau_{in}$ obtained from magnetoresistance data,[26,27,32] which is comparable to the theoretically predicted $1/\tau_{e-e}$.[33] As pointed out by Gordon, Lobb, and Tinkham,[22] the equivalence of $1/\tau_\phi$ and $1/\tau_{in}$ does not hold near T_c. Since $1/\tau_{in}$ determined from magnetoresistance includes primarily electron-electron and electron phonon scattering rates, the divergence of δ shown in Fig. 5 is an indication of this nonequivalence. In the case of Nb, the large spin-orbit scattering rate ($1/\tau_{so}$) further complicates the analysis. Because of its Z^4 dependence, where Z is the atomic number, it is hard to determine $1/\tau_{so}$ accurately. While spin-orbit scattering does not pair break,[33] i.e., it does not change δ, it significantly affects the magnetoresistance. To obtain $1/\tau_{in}$, it is customary to first assume a $1/\tau_{so}$ value independent of temperature and then fit the experimental data to the theoretical function, which depends on the combination $1/\tau_{in}+4/3\tau_{so}$.[27,32] Hence the uncertainty in the value of τ_{so}, ranging from 10^{-14} sec (Ref. 27) to 2×10^{-12} sec for Nb,[34] could introduce an error in $1/\tau_{in}$. It is uncertain that this is the reason for the discrepancy between τ_ϕ obtained from fluctuation-conductivity analysis and τ_{in} obtained from magnetoresistance measurements. We should also mention that for Al, which is a light element, the complication of spin-orbit scattering is not present and the equivalence of $1/\tau_\phi$ and $1/\tau_{in}$ well above T_c has been demonstrated.[2,22]

Figure 5 shows that the increase in δ vs T slows down at higher temperatures. Far away from T_c, superconducting fluctuations are unstable, making Eq. (19) inapplicable. In addition, since σ'_{AL} can be derived from GL formalism, valid only close to T_c, Eq. (10) is not exact as $T\rightarrow 2T_c$, and one cannot truly trust the values of δ for $\tau \gtrsim 0.5$.

C. Effect of magnetic fields

Theoretical understanding of the fluctuation conductivity in finite fields is rather poor compared to that in zero field, and comparison with experiments has not been widely tested. For large perpendicular fields, calculations showed that, near $T_c(H)$, the AL contribution is $\sigma'_{AL}(H_\perp)=4\sigma'_{AL}$ ($H=0$). This enhancement is due to the degeneracy of the ground state of the quantized Landau orbits produced by perpendicular fields.[35] The MT contribution is suppressed because δ now includes the pair-breaking strength due to external fields. In the pair-breaking language,[12] δ has two terms:

$$\delta(H)=\delta(H=0)+\frac{2e\xi^2(0)}{\hbar c}H$$
$$=0.18+3\times10^{-5}H\ , \qquad (11)$$

for perpendicular fields, where H is given in oerstead. As mentioned, above the larger δ, the smaller the contribution of σ'_{MT} is.

Figure 7 plots the normalized $1/\sigma'$ as a function of T for the Nb film in $H_\perp=0$, 2, 5, and 8 kG, as well as σ'_{AL} and $4\sigma'_{AL}$. As the field increases, the curvature of $1/\sigma'$ vs T near $T_c(H)$ changes sign, and the slope increases toward that of the AL contribution alone. For $H=8$ kG [$\delta=0.42$ according to Eq. (11)], $4\sigma'_{AL}$ is always larger than σ'_{MT} from T_c to $2T_c$. The experimental result near $T_c(H)$ seems to agree with $4\sigma'_{AL}$. Although the agreement is not complete, as seen in the departure of the experimental data from the theory, the behavior near T_c as a function of field convincingly shows that the MT contribution is being suppressed by the external fields.

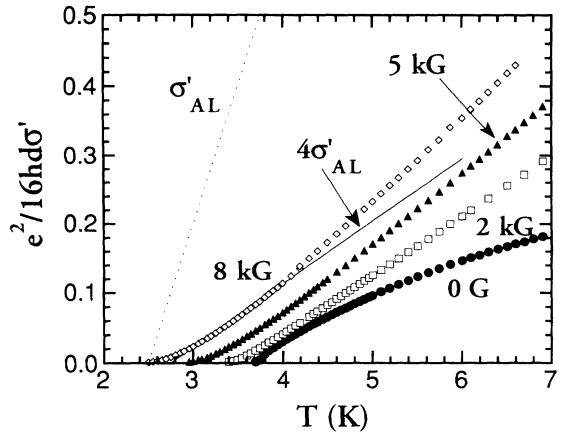

FIG. 7. Normalized inverse fluctuation conductivity as a function of temperature for various perpendicular fields.

In conclusion, because of the "cleanliness" (long l) and the crystallinity of the sample, the zero-field fluctuation conductivity can be understood when taking into account both AL and MT contributions. The pair-breaking parameter obtained is in agreement with other reported values of polycrystalline Nb films. The determined pair-breaking rate is larger than the inelastic electron-electron scattering rate alone. This discrepancy is not fully understood, but it could be caused by the complication of large spin-orbit scattering in Nb. Results of perpendicular-field fluctuation conductivity show that pair breaking introduced by a magnetic field destroys the MT contribution so that the AL term alone is sufficient to explain the data.

IV. DEVELOPMENT OF RESISTIVE TAILS IN LOW MAGNETIC FIELDS

A. Kosterlitz-Thouless transition in thin-film superconductors

In a 2D solid, no long-range positional order can be found at any $T>0$ because of the long-wavelength thermal fluctuations of the lattice. However, it was discovered by Kosterlitz and Thouless that a new type of long-range order (topological order) exists at low temperatures even though the positional order is short ranged. A nonzero transition temperature T_{KT} was found, above which the long-range topological order is also destroyed. The critical behavior near T_{KT} displays very weak singularities; in contrast to the first- or second-order phase transitions, all derivatives of the free energy are finite and bounded at T_{KT}.[36] The essential point of the Kosterlitz-Thouless transition lies in the fact that the interaction potential (U) depends logarithmically on the distance.

In a neutral superfluid, no free vortices exist below T_{KT} because the energy required to create a vortex is proportional to $\ln(L)$, where L is the size of the sample. Even though $\ln(L)$ is large for macroscopic samples, the energy required to generate a vortex-antivortex bound pair is rather small, $\propto \ln(r)$, where r is the size of the pair; thus bound pairs exist with probability $\exp(-U/kT)$ at $T\neq 0$. These bound pairs dissociate into free vortices at T_{KT}. It was originally thought that the KT transition could not be observed in superconductors, because λ cuts off the range of the interaction potential. Therefore, the energy required to create a vortex in a superconductor is always finite, $\propto \ln\lambda$, independent of sample size; consequently, free vortices exist in 2D superconductors at all $T>0$.[36] However, this picture is modified for superconducting films with thickness $d<\lambda$, where Pearl showed that the interaction energy between two vortices is

$$U=\begin{cases}\left[\dfrac{\Phi_0}{2\pi\lambda}\right]^2 d\left[\ln\dfrac{\lambda}{r}+\ln\dfrac{4\lambda}{d}-\gamma\right], & r\ll 2\lambda_\perp \\ \left[\dfrac{\Phi_0}{2\pi}\right]^2\left[\dfrac{1}{r}\right], & r\gg 2\lambda_\perp ,\end{cases} \tag{12}$$

where γ is the Euler's constant.[37] As shown in Eq. (12), $\lambda_\perp$ replaces λ in thin films. Beasley, Mooij, and Orlando (BMO) then realized that $\lambda_\perp$ can be of the order of mm to cm for dirty superconductors,[38] so that one can easily have samples whose smallest dimension is much less than $\lambda_\perp$. Hence there is no difference between superconductors with $w\ll\lambda_\perp$ and superfluid ^{4}He of finite sample size; in both systems, the KT transition is broadened because a few free vortices coexist with bound vortex-antivortex pairs below T_{KT}, but all bound pairs still dissociate spontaneously at T_{KT}.

Extending the theory developed for superfluid ^{4}He films to superconductors, BMO found that

$$kT_{KT}=\frac{\Phi_0^2}{32\pi^2}\frac{1}{\lambda_\perp(T_{KT})} . \tag{13}$$

In the dirty limit, they showed that T_{KT} is lower than the CS transition temperature T_c by an amount depending on $R_\square$. Equation (13) becomes

$$T_{KT}\simeq\frac{T_c}{1+0.173R_\square/R_c}\simeq T_c\left[1-0.173\frac{R_\square}{R_c}\right], \tag{14}$$

where $R_c\equiv\hbar/e^2=4.11\ \text{k}\Omega/\square$. To clearly observe a T_{KT} below T_c requires a sample with large $R_\square$, $\gtrsim 1\ \text{k}\Omega$.[38] Since free vortices will be swept across the sample by bias currents and hence cause dissipation, thin-film superconductors exhibit finite resistance for $T_{KT}<T<T_c$. Although the R-vs-T curves are smooth and continuous at T_c, this is the temperature where the superconducting gap actually closes; i.e., the order parameter exists above T_{KT} up to T_c, and this T_c should agree with the T_c determined from analysis of the fluctuation conductivity (Sec. III).

Halperin and Nelson further studied the resistive transition in superconducting films by combining a GL phenomenological picture with the analog of the theoretically predicted jump in the superfluid density or neutral superfluids.[9] Interpolating between fluctuation conductivity (σ') above T_c and the results for the KT transition in superfluid ^{4}He below T_c Halperin and Nelson arrived at

$$\sigma' \simeq 0.37 b^{-1} \sigma_n \sinh^2(\sqrt{b\tau_c/\tau}) , \quad (15a)$$

where b is a dimensionless number of order unity, σ_n is the normal-state conductivity, $\tau \equiv (T-T_{KT})/T_{KT}$, and $\tau_c \equiv (T_c-T_{KT})/T_{KT}$. Their formulation is valid for both $0<\tau \ll \tau_c$ $(T_{KT}<T \ll T_c)$ and $\tau_c \ll \tau \ll 1$ $(T_c \ll T \ll 2T_{KT})$. For $T \gg T_c$ $(\tau \gg \tau_c)$, $\sqrt{b\tau_2/\tau} \ll 1$, and Eq. (15) becomes

$$\sigma' \simeq \frac{0.37}{b}\sigma_n \left[\frac{b\tau_c}{\tau}\right] \simeq 0.37\sigma_n \left[\frac{T_c-T_{KT}}{T-T_{KT}}\right] , \quad (15b)$$

reproducing σ'_{AL} [Eq. (5)] when T_{KT} is eliminated using Eq. (14). Only the AL contribution was considered because the MT term is negligible for dirty superconductors and BMO theory concerns this limit only. In the other temperature region $\tau \ll \tau_c$ (i.e., near T_{KT}), $\sigma \approx \sigma' \gg \sigma_n$, and

$$\frac{R}{R_n} \simeq 10.8b \exp(-2\sqrt{b\tau_c/\tau}) \quad (16)$$

is due to the motion of the unbound vortices under applied currents.

Since the KT transition is analogous to a 2D Coulomb gas, the resistive transitions of different superconductors should be governed by the same universal curve after rescaling the material parameters, such as T_c, T_{KT}, R_n. Analyzing the R-vs-T data for granular Al, amorphous Nb_3Ge, amorphous Bi, and a planar array of Pb-Sn Josephson junctions with T_c's ranging from 2.2 to 6.1 K, Minnhagen found that scaling behavior is possible and the R/R_n curves are a function of X only,[39] where

$$X = \frac{T}{T_c-T}\frac{T_c-T_{KT}}{T_{KT}} .$$

Although the actual functional dependence of R/R_n on X is unknown theoretically, one can follow Minhagen's prescription to determine T_{KT} and T_c. This analysis was also done on He-Xe (Ref. 39) and In/InO_x (Ref. 40) films, yielding reasonable agreements.

From the theoretical discussion, it is obvious that a few conditions must be satisfied in order to observe the KT transition in thin-film superconductors: (1) The width of the sample should be smaller than its $\lambda_\perp$, (2) H is sufficiently small, and (3) vortex-pinning effects ought to be weak. The first point has been discussed in detail before: The interaction potential between vortices has a logarithmic dependence to length scale $\approx \lambda_\perp$. In addition, the greater the $R_\square$ is, the larger the separation between T_{KT} and T_c is.

The measured resistance in a field $H > H_{c1}$ is proportional to the total number of free vortices present, including contributions from both injected vortices and unbound pairs.[41,42] Furthermore, since it is energetically more favorable to have vortices than antivortices in a field, the external field can induce pair unbinding below T_{KT}.[42] Hence, to ensure that the R/R_n value measured is due to the Kosterlitz-Thouless transition, i.e., from the unbinding of vortex-antivortex pairs above T_{KT}, one must perform the measurement in sufficiently low external fields.[41]

Although all theoretical models developed do far have not considered the effect of pinning, pinning is unavoidable experimentally, especially when a high-resistance sample is involved.[38] Suppose a vortex of a bound pair is situated at a pinning site; under the influence of bias currents, it might be more favorable for the pinned vortex not to move and to break up the pair than for the pair to remain intact. Therefore, in the presence of pinning, additional unbinding of vortex-antivortex pairs and trapping of free vortices can cause the temperature dependence of the resistance to be modified. All these factors complicate the analysis of experimental results.

B. Experimental results and analysis

We found that the data on resistance tails in low fields ($\lesssim 20$ G) were unexplainable by flux-creep theory; $\ln(R/R_n)$ plotted as a function of $1/T$ shows significant nonlinearity at the higher-temperature part of the transition, but well below the midpoint of the transition, i.e., $R \lesssim 0.5R_n$. (See Fig. 8). Since our sample is a 2D superconductor, it is reasonable to consider the possibility of the KT transition, which predicts a nonthermally activated temperature dependence in resistance curves. Figure 9 shows R/R_n as a function of temperature for data taken in a shielded Dewar. The solid line is a fit of the data to Eq. (16) with fitted values $b=1.02$, $T_{KT}=3.60$ K, and $T_c=3.77$ K, which agrees reasonably with the T_c obtained from fitting the fluctuation conductivity ($=3.725$ K). Similar discrepancies in T_c obtained from fluctuation-conductivity and Kosterlitz-Thouless analyses have been observed previously,[43] but one can see that there is a resistive tail whose temperature dependence cannot be described by KT theory. We discuss this point further below.

Another method used to analyze the KT transition is Minnhagen's empirical universal resistance curve. The procedure is (1) read off X values for corresponding

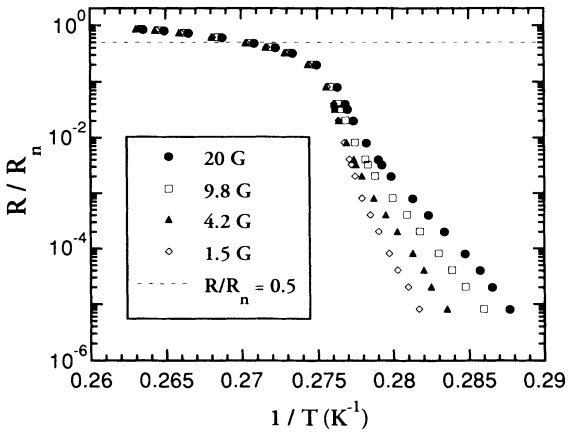

FIG. 8. R/R_n (logarithmic) vs $1/T$ for low fields.

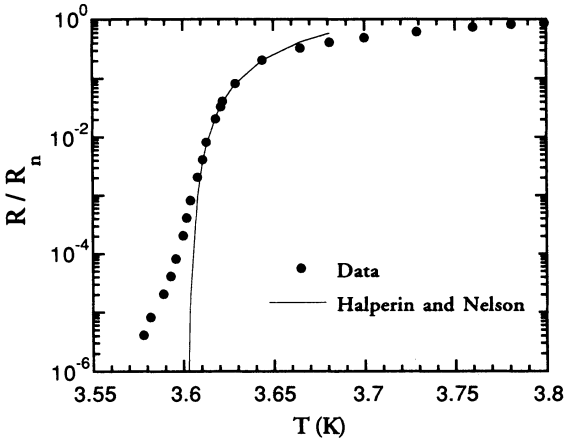

FIG. 9. R/R_n (logarithmic) vs T for zero applied field in a shielded Dewar. The solid line is a fit to Eq. (16) with $b=1.02$, $T_{KT}=3.60$ K, and $T_c=3.77$ K.

R/R_n values from the universal curve in Ref. 39, (2) obtain the temperature values from the data (Fig. 9) for the same R/R_n values and (3) a linear relation should exist between T/X and T because

$$\frac{T}{X}=\frac{T}{\left[\frac{T}{T_{KT}}\frac{T_c-T_{KT}}{T_c-T}\right]}=\left[\frac{T_{KT}}{T_c-T_{KT}}\right](T_c-T)\,. \tag{17}$$

We obtained and plotted T/X vs T in Fig. 10; the linear relation is quite evident. The experimental data extrapolates to the temperature axis, i.e., $T/X=0$, at T_c. T_{KT} is determined by the intercept of $T/X=T$ (dashed line) and the experimental result (solid line). This method produces $T_c=3.66$ K and $T_{KT}=3.565$ K; both are lower than the values obtained from fitting the R-vs-T curve with the Halperin-Nelson model. Considering that the

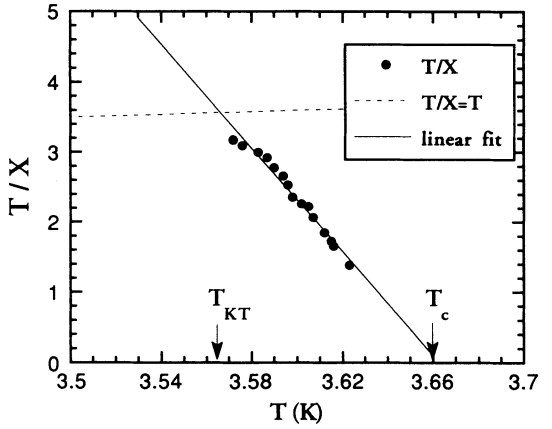

FIG. 10. T/X vs T. The solid line is a linear fit to the experimental data, and the dashed line is $T/X=T$. Their intercept gives the valence of T_{KT}. T_c is determined by $T/X=0$. Both $T_{KT}=3.565$ K and $T_c=3.66$ K are indicated in the figure.

universal curve was obtained from very different materials and its generality is still under investigation, we do not consider the difference between the two T_{KT} values (≈ 35 mK) to be significant. Note that T_c, obtained from fluctuation-conductivity analysis, where $R\sim R_n$, is in between the two values obtained from the KT region where $R\ll R_n$. Perhaps both the Halperin-Nelson and Minnhagen models are insensitive to T_c.

Next, we would like to discuss the validity of applying existing models for the KT transition in dirty superconductors to our Nb film, which is a clean system. Using the measured $R_\square=122\ \Omega/\square$ and Eq. (14), we estimate $T_{KT}/T_c\approx 0.995$, corresponding to $T_c-T_{KT}\approx 20$ mK, agreeing fairly well with the experimental results mentioned above. Since the width of the sample, $w=96\ \mu$m, is a few times $\lambda_\perp(T=0)\approx 13\ \mu$m and the KT transition is expected only when $\lambda_\perp(T)>w$, the temperature region for which KT theory applies exists only very near T_c. Using Eq. (2), we find that $\lambda_\perp(T)\gtrsim w$ for $T\gtrsim T^*\approx 3.23$, K, making it possible that we observed evidence of the KT transition at low fields near T_c. The presence of strong pinning (see next section) complicates matters; pinning might be the cause of resistance deviating from the KT temperature dependence at zero field. In addition, only the AL contribution to σ' was included in the calculation of Halperin and Nelson, but the MT term was also required to analyze the fluctuation conductivity in our clean 2D Nb film. The effect of the MT term on the KT transition is currently unknown. Therefore, it is reasonable, though not conclusive, to say that the KT transition has been observed in our system. The major difference between our system and previous work on the KT transition in superconducting films is that existing studies, e.g., In/InO_x (Ref. 40) and granular Al,[44] have been on dirty superconductors with the mean free path limited by disorder.

When a small perpendicular field is applied, a tail (i.e., excess resistance) with a thermally activated temperature dependence becomes evident at low temperatures (see Fig. 11), very similar to that of Garland and Lee[40] (see Fig. 9 of Ref. 40) and the prediction of Doniach and Huberman.[42] The temperature at which the resistance curves deviate from the zero-applied-field curve increases as field increases. The temperature region where the KT temperature dependence was observed vanishes at 10 G. The remnant field in the shielded Dewar was quoted as <30 mG because an external field of $\lesssim 30$ mG caused no deviations from the zero-applied-field case. It may be that the deviations occur at very small R below our experimental resolution. As mentioned above, there exists a tail, even at zero applied field, which does not have the KT temperature dependence. This tail could be caused by the remnant field, but it is also possible that it is intrinsic to the sample, perhaps as a result of pinning unbinding of the vortex-antivortex pairs.

In summary, evidence of the KT transition was observed in a 2D single-crystal Nb film, even though it is a clean system with strong pinning. The apparent KT transition signature disappears when a sufficiently large perpendicular field is applied, where thermally activated

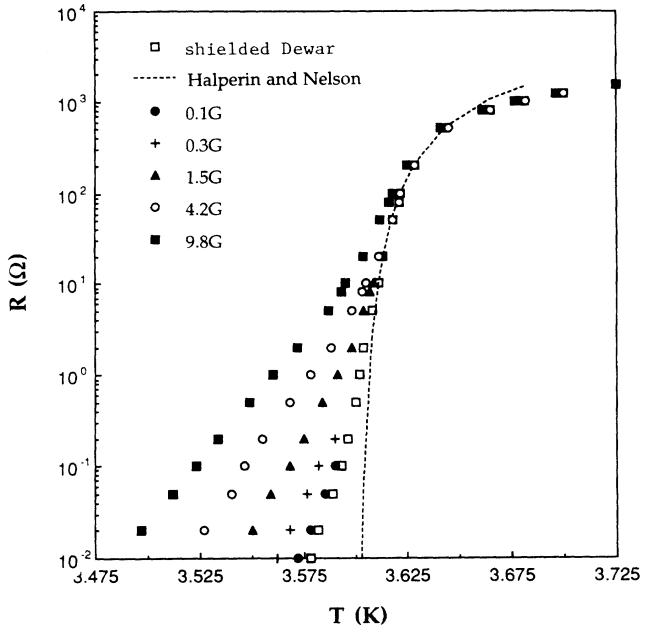

FIG. 11. R/R_n (logarithmic) vs T for low fields.

flux motion becomes the dominant contribution to the resistance.

V. FLUX-CREEP REGIME

A. Background

When a superconductor is placed in a field, pair-breaking effects suppress T_c; thus bulk conventional superconductors show a T_c reduction with little broadening of the transition width, defined as the temperature difference between 10% and 90% R_n. This is untrue in thin-film superconductors[5,23] and in recent measurements on the cuprate superconductors. Figure 12 is a plot of R vs T in various perpendicular fields for the 2D Nb film.

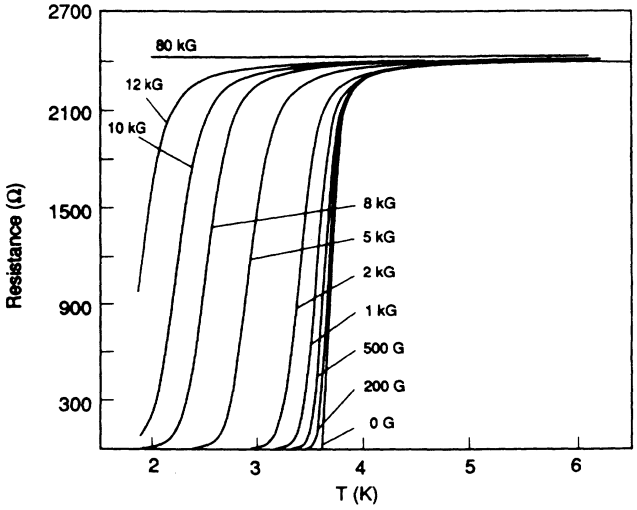

FIG. 12. R-vs-T curves, in various perpendicular magnetic fields, of a 20-Å Nb film.

Below 1 kG, a tail develops at the "foot" of the transition ($\lesssim 10$)% R_n), while the "top" (90% R_n) of the transition (fluctuation region) shows very little change, similar to the resistive transition of the high-T_c cuprate superconductors.[45,46] However, unlike the high-T_c materials, at higher fields ($H \gtrsim 2$ kG), the transition curves shift down in temperature as well as broaden in transition width. As we are only concerned with the resistive tails in perpendicular magnetic fields, we shall explain our results in the framework of thermally activated flux-motion (flux-creep) theory. Therefore let us first review the simple Anderson-Kim model of flux creep,[47] which was worked out for 3D conventional superconductors. We will extend the model to two dimensions and apply it to our 2D system.

In order to minimize the free energy, magnetic-field lines penetrate type-II superconductors when $H_{c1} < H < H_{c2}$. The Anderson-Kim model applies for $H_{c1} \ll H \ll H_{c2}$, where $B \approx H$. The original theory also assumed that λ is much larger than the distance between the flux lines $a_H \approx \sqrt{\Phi_0/H}$, where $\Phi_0 = 2\times 10^{-7}$ G cm^2 is the flux quantum. Since it is energetically unfavorable to have perturbation in flux-line density of length scale $< \lambda$, a local Abrikosov flux lattice of size λ forms. Anderson argued that this local lattice must remain intact and called it a "flux bundle,"[48] containing $(\lambda/a_H)^2$ flux lines. For films with $d < \lambda$, vortices form in the superconductor with circulation currents extending to $\lambda_\perp$, increasing the dimension of the flux bundle from λ to $\lambda_\perp$. On the other hand, the interaction energy between the vortices is proportional to the length of the vortices,[37] which is greatly reduced when a superconductor is made thin. Thermal fluctuations cause instability in the Abrikosov lattice; thus, at a finite temperature T_M, well below T_c, the vortex lattice is no longer capable of supporting stress induced by thermally excited dislocation pairs and the vortex lattice is said to melt. For $T > T_M$, vortex motion is uncorrelated,[49,50] and we should consider individual vortices instead of flux bundles.

In the absence of pinning sites, such as crystal defects, cavities, impurities, etc., an applied current ($\mathbf{J}$) would impose a Lorentz force per unit volume, $(\mathbf{J}\times\mathbf{H})/c$, on the flux lines, resulting in flux motion, which in turn causes dissipation. (c is the speed of light.) Hence, in a perfect material, a true superconducting state (i.e., zero resistance) can only exist at zero bias current or zero field, but in reality pinning sites always exist. One can view pinning centers as potential minima where vortices prefer to be. At zero temperatures, if the external Lorentz force is not "large enough," the vortices remained pinned and no resistance (dissipation) is observed for current density $J < J_c$, the value of J at which the Lorentz force is large enough to observe resistance.

For $T > 0$, there is always a finite probability of vortices jumping from one pinning site to another. As mentioned above, in the case of 3D superconductors, because it is energetically unfavorable to disturb the Abrikosov lattice on a length scale smaller than λ, an individual flux line cannot jump by itself; rather, the whole flux bundle jumps as a unit. Since this energetic argument does not

apply to the 2D case when the vortex lattice is melted, motion of an individual vortex is possible. Let F_0 be the "activation free energy," the minimum free energy gained by the system so that vortices can overcome the barrier between two local potential minima. The jump rate is thermally activated, i.e.,

$$f=f_0\exp\left[\frac{-F_0}{kT}\right], \tag{18}$$

where f_0 is some characteristic frequency whose exact value is unknown, but is estimated to be $\sim 10^5-10^{10}$/sec,[47] and k is the Boltzmann constant. The flux-creep regime is where $F_0 \gg kT$. Even though $f\neq 0$ at $T\neq 0$, these jumps occur in all directions in the absence of external applied currents and the average creep velocity $v\equiv fL$ equals zero. When a current is passed through the superconductor, it induces a flux-density gradient; i.e., the potential now looks like a tilted washboard.[11] Thus it is easier for vortices to move in the direction of the potential gradient (i.e., in the direction of $\mathbf{J}\times\mathbf{H}$) than to move against it. The net jump rate is then

$$\begin{aligned} f&=f_+-f_- \\ &=f_0\exp\left[\frac{-F_0}{kT}\right]\left[\exp\left[\frac{\Delta F}{kT}\right]-\exp\left[\frac{-\Delta F}{kT}\right]\right] \\ &=2f_0\exp\left[\frac{-F_0}{kT}\right]\sinh\frac{\Delta F}{dT}, \end{aligned} \tag{19}$$

where the contribution, due to the Lorentz force,

$$\Delta F=\frac{JHVL}{c}, \tag{20}$$

with V being the flux-bundle volume and L the hopping distance. (L will be estimated in Sec. V C.) Since we are interested in thermally activated flux motion and not in the Lorentz-induced flux motion, we use bias currents so that $\Delta F/kT \ll 1$. Expanding to the first order of sinh, the creep velocity

$$\begin{aligned} v&\equiv fL \\ &\approx 2f_0L\left[\frac{JHVL}{kT}\right]\exp\left[\frac{-F_0}{kT}\right], \end{aligned} \tag{21}$$

and the induced electric field $E=B(v/c)$, which is proportional to J, i.e., Ohmic. (This point will be discussed further in Sec. V C.) In this case we define a flux-creep resistivity

$$\rho=\frac{E}{J}=\frac{2f_0H^2VL^2}{c^2kT}\exp\left[\frac{-F_0}{kT}\right]. \tag{22}$$

Because of the uncertainties in values and field dependences of f_0, V, and L, we write the flux-creep resistance as

$$R=f(H)\exp\left[\frac{-F_0}{kT}\right], \tag{23}$$

where $f(H)$ is some function of the applied field, which increases as H increases.

Next, we shall estimate F_0. In the most general case,

$$F_0(T,H)=U(T,H)-TS_{\text{eff}}(T,H), \tag{24}$$

where $U(T,H)$ is the barrier energy and S_{eff} is the effective entropy, which is related to the curvature of the pinning potential at the local maxima.[51] The exact value of S_{eff} cannot be known unless detailed knowledge of the pinning potential is available. In the original Anderson-Kim model, they argued that

$$F_0\approx U=p\frac{H_c^2}{8\pi}\xi^3, \tag{25}$$

where H_c is the thermodynamic critical field, ξ is the superconducting coherence length, and p is the effective factor, a small number. This assumes core pinning in a bulk superconductor, such as a defect or void of the size ξ^3. The system can gain the whole condensation energy $(H^2/8\pi)$ by placing a vortex core at the defect. Yeshurun and Malozemoff recently proposed that, for $\lambda \gg a_H$, ξ^3 in Eq. (25) should be replaced by $a_H^2\xi$; that is, collective effects in pinning become important as field increases.[52] F_0 given by Eq. (25) is usually large, of the order of ~ 1 eV, and so at low temperatures of flux-creep resistance is immeasurably small in bulk conventional superconductors. Another important point is that F_0 in Eq. (25) goes to zero as $\sqrt{1-t}$ as T approaches T_c, where $t=T/T_c$. In general, F_0 should always decrease to zero at T_c as some power of $(1-t)$. Since the flux-creep regime is where $F_0 \gg kT$, the theory fails very near T_c when $F_0(T)$ becomes comparable to kT.

For 2D superconducting films, we argue that ξ^3 in Eq. (25) should be replaced by $\pi\xi^2 d$ because vortices are disks of thickness d. In addition, the condensation energy should be replaced by the line energy (ε).

$$\varepsilon=\pi\xi^2 d\left[\frac{H_c^2}{8\pi}\right]+\left[\frac{\Phi_0}{4\pi\lambda}\right]^2 d\left[\ln\frac{\lambda}{\xi}+\ln\frac{4\lambda}{d}-\gamma\right], \tag{26}$$

with contributions from both the core (the first term) and the circulating currents (all the other terms), where γ is the Euler constant.[37] Because of the exponential nature of the flux-creep resistance [Eq. (23)], it is only measurable when F_0/kT is of the order of 1–10. In the recently discovered cuprate superconductors, T_c is ~ 100 K instead of ~ 10 K and F_0 is not large because of their quasi-2D nature. Hence flux creep is important to the transport properties in these systems, as was pointed out by Tinkham.[53] In 2D superconducting films, the line energy decreases linearly as d decreases for films with $d<\xi$.[37] Since the activation energy needed to overcome a pinning potential is a fraction of the line energy, the maximum possible activation energy should be much smaller for a thin film than for a bulk sample. In a single-crystal two-dimensional film where the density of crystalline defects is low, this reduction of the zero-temperature pinning energy will allow vertex motion to be evident, as will be evident in the 2D Nb film.

B. Experimental results and analysis

To study resistive tails in the 2D single-crystal Nb film in detail, we measured the resistive transitions in perpendicular magnetic fields from 0.1 G to 8 kG. Figure 13 shows R/R_n displayed in a semilog plot as a function of $1/T$ for the tails of the transitions in perpendicular magnetic fields. $R/R_n=0.5$ is indicated. The linear proportionality over four decades in resistance from $0.5R_n$ down to our experimental resolution $\lesssim 10^{-5}R_n$ of $\ln(R/R_n)$ to $1/T$ strongly suggests that the dissipation mechanism is thermally activated. We should note that thermally activated resistance was not seen when we measured a 1600-Å Nb film ($T_c=8.79$ K) made the same way.

Within the model of flux creep, i.e., $\ln R \propto -U/T+\beta$, the activation energy U in general depends on both temperature and field. However, our data shows no deviation from linearity of $\ln R$-vs-$1/T$ curves (Fig. 13); thus U in the 2D Nb system must either be temperature independent or contain at most a linear correction, i.e., $U(T,H)=H_0(H)-a(H)T$. Since the activation energy is proportional to the vortex-core energy plus magnetic energy, for a 2D superconductor $U(T)\propto(\Phi_0/4\pi\lambda)^2 d$, whose dominant temperaure dependence is $1-t$ near T_c; thus we believe that a linear temperature dependence of U would be the likely case in this system. Therefore, we fit the thermally activated part of the data with

$$\frac{R(H)}{R_n}=f(H)\exp\left[-\frac{U_0(H)}{kT}+K(H)\right], \tag{27}$$

where $U_0(H)$ is the field-dependent zero-temperature activation energy, $K(H)$ includes $a(H)$ as well as an effective entropy term,[54] and $f(H)$ is chosen to be H/H_{c2}, which is proportional to the number of injected vortices.[42,50,55] Table I lists the values of $U_0(H)$ and $K(H)$ for all fields. The inclusion of $K(H)$ in our analysis is essential; attempting to treat $\exp(K(H))$ as the prefactor would result in an unphysically large prefactor,

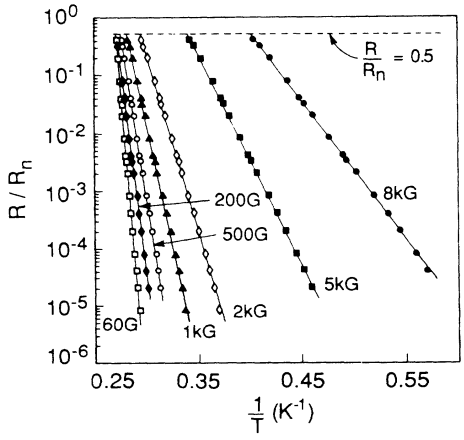

FIG. 13. Normalized sheet resistance R/R_n (logarithmic scale) vs $1/T$ for different applied magnetic fields. The dashed horizontal line indicates the midpoint of the transition, $R/R_n=0.5$. The solid lines are fit to the data using Eq. (27).

TABLE I. Values of H, $U_0(H)$, and $K(H)$ for a 2D single-crystal Nb film.

H (G)	$U_0(H)$ (K)	$K(H)$
0.1	1790	501
0.3	1386	388
1.5	1220	342
4.2	995	279
9.8	799	224
19.5	697	196
60	500	141
97	468	132
100	436	123
200	344	97.7
500	267	76.8
800	223	65.3
1000	199	58.6
2000	148	45.4
5000	85.5	30.0
8000	54.9	22.4

which decreases as field increases, contradicting the theoretical model discussed in the previous section. Experiments on other 2D superconducting films, e.g., granular Al,[3] MoGe,[4] In/InO_x,[40] also showed the existence of $K(H)$ in these systems.

To further understand the pinning mechanism in our sample, Fig. 14(a) shows $U_0(H)$ and $K(H)$ vs H in a log-log plot. $U_0(H)$ data of a $Bi_2Cr_2CaCu_2O_8$ (Bi-Sr-Ca-Cu-O) single crystal as obtained by Palstra *et al.*[46] are presented in Fig. 14(b). One immediately notices the similarities between the two systems: U_0 decreases as $H^{-\alpha}$, with $\alpha\simeq\frac{1}{6}$ at low fields and $\alpha\simeq\frac{1}{3}$ at higher fields. Nevertheless, we should point out that the data on Bi-Sr-Ca-Cu-O cover only two decades in field while the Nb data cover five decades. With this wider range of fields, it is apparent that power-law dependence of $U_0(H)$ seem unconvincing. Recently, flux-creep models involving a distribution of pinning energies have been proposed to understand the field dependence of $U_0(H)$ in the cuprate superconductors.[56,57] Analyzing $U_0(H)$ from our data within the model of an exponential or Gaussian distribution of pinning energies produces reasonable, though inconclusive, results for low fields ($H<20$ G), but these models cannot explain the entire range of our $U_0(H)$. (See Fig. 15). Another interesting feature of Fig. 14 is that $U_0(H)$ is of the same order of magnitude for both systems, despite T_c being 20 times higher for Bi-Sr-Ca-Cu-O. The data for the 2D Nb above 2 kG can be explained by crossover from individual flux pinning to collective pinning. We shall discuss these points below.

Since the Nb film is a single crystal, pinning due to crystalline defects should be negligible. Also, since the width of the sample is much larger than $\lambda_\perp$, we do not expect edge pinning to play an important role. However, thickness variations (Δd) due to the roughness of Nb/α-si and Nb/sapphire interfaces could generate significant pinning potential. Atomic-force microscope (AFM) images[58] of similar substrates show that off-axis polishing

produces regular steps of 4±1 Å in height and 500–2000 Å in separation. This could cause a thickness variation in the 20-Å Nb film of 10–20%. Assuming that thickness variations are the main source of pinning, we estimate the activation energy by calculating the energy gained by a vortex sitting on a thinner spot. Including both the core and magnetic terms given by Pearl,[37] we estimate the pinning energy due to a 4-Å thickness variation to be at most 1800 K, very close to the experimental observed values at low fields. Of course, this estimate is very crude because we have neglected the interaction between vortices.

Because the c-axis coherence length is extremely short ($\xi_c < 2$ Å) in the Bi-Sr-Ca-Cu-O system, instead of a rodlike structure, a vortex in this system is better described as a stack of disks whose thickness is characterized by ξ_c. Thus the similar values for $U_0(H)$ obtained for that system[46] could be understood in this simple picture with Δd replaced by ξ_c.

As Fig. 14(a) shows, $U_0(H)$ from the 2D Nb data exhibits a field dependence stronger than $H^{-1/3}$ for $H \gtrsim 2$ kG. A field of 2 kG corresponds to a distance between vortices, $a_H \approx \sqrt{\Phi_0/H} \approx 1000$ Å, which is of the same order as the periodicity of the sapphire steps

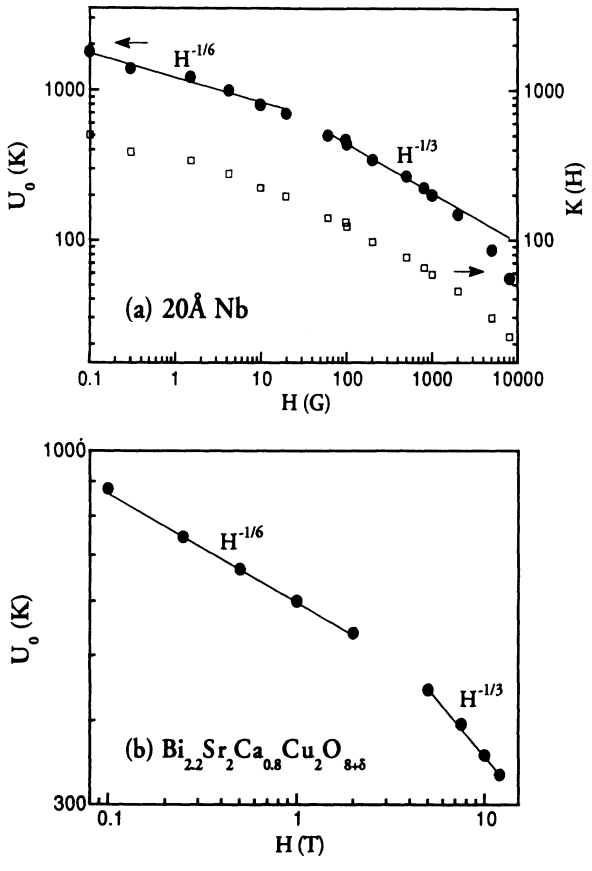

FIG. 14. $U_0(H)$, in units of kelvin (K), vs H in log-log scale. (a) Data for a 2D Nb single-crystal film (this work). $K(H)$ [Eq. (27)] is also shown using vertical scale on the right. (b) Data for a Bc-Sr-Ca-Cu-O single crystal (Ref. 46). Solid lines show the power-law dependence for limited-field regions.

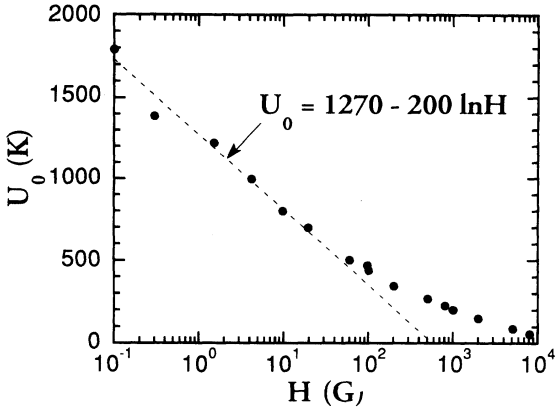

FIG. 15. U_0 vs H (logarithmic) for 2D Nb. The dotted line is the thoeretical model for an exponential distribution of activation energies.

(500–2000 Å). Hence, at high fields, where the density of vortices is higher than that of pinning sites, pinning of a vortex bundle becomes more important than pinning of an individual vortex. In this limit it has been argued that $U_0(H)$ decreases as $1/H$,[53,52] agreeing qualitatively with our experimental observation.

C. Current-voltage relation

We measured I-V curves at various temperatures for different fields. Figure 16 shows I-V curves for data taken in the shielded Dewar. Results in finite fields are qualitatively the same.

(1) In the temperature region where we observed thermally activated resistance, V is linearly proportional to I for small current. The value of V/I in the limit of $I \rightarrow 0$ is the resistance measured in the R-vs-T curve. As the current is increased, V grows faster than I in order to cross over the normal-state I-V curve, where $V = R_n I$.

(2) For temperatures much lower than the region where finite resistances can be measured, we observe critical currents. The inset of Fig. 16(b) shows the current (I_c) at which voltage starts to appear as a function of T.

Two conclusions emerge from these I-V data. First, even at the lowest fields, we do not see the nonlinear I-V predicted by KT theory [$I \propto V^{a(T)}$, where $a(T) \gtrsim 3$ for $T \lesssim T_{KT}$]. Since all results of KT theory are worked out for the case of no pinning, the existence of pinning might be the cause of apparant critical currents observed in the low-temperature region. Moreover, we did not observe any classical flux-flow regime,[55] where $R/R_n = H/H_{c2}$. When the temperature is high enough that we can measure a resistance at low currents, the I-V curves start out to be linear, representing flux-creep behavior ($V \propto \sinh I$), and then cross to the normal state. In fact, attempts to fit these I-V curves with a flux-creep to flux-flow model[59] result in a fitted flux-flow resistance equal to R_n. Results from R-vs-H measurements for $T \lesssim T_c$ also confirm that a classical flux-flow regime does not exist in our 2D Nb film. Figure 17 shows resistance as a function of perpendicular field. The classical flux-flow region should show a linear relation between R and H, but no such linear R-

vs-J region is present in Fig. 17.

Recently, a vortex-glass–liquid phase-transition model was proposed to explain the behavior of high-T_c cuprate superconductors.[60] Because of the two dimensionality of the ultrathin Nb film, the vortex structure in the mixed state is in the liquid phase for all finite temperature; i.e., the glass transition temperature is at $T=0$ for 2D systems. In this model a vortex-hopping distance L_{VG} is defined as

$$\left[\frac{J_c^{(2D)}\Phi_0}{c}\right]L_{VG}=kT\ , \tag{28}$$

where $J_k^{(2D)}\equiv I_c/w$ is the 2D current density at which the I-V curves deviate from linearity. Vortices can hop because the potential energy due to the Lorentz force on a single vortex [the left side of Eq. (28)] is supplied by the thermal energy kT.[61] If $L_{VG}<\sqrt{\Phi_0/H}\approx a_H$, the individual vortex-hopping picture is valid. Figure 18 shows L_{VG} vs T determined from the I-V curves near T_c for $H=200$ G, 2 kG, and 5 kG, $J_c^{(2D)}$ was defined as the current density at which the resistance (V/I) equals twice the resistance in the low-current limit. This definition is quite crude, but it is sufficient for the purpose of showing that, for the temperature range in which we observed flux-creep behavior, L_{VG} is always $\lesssim a_h$ for fields $H\lesssim 2$ kG. Hence collective pinning is only important for $H\gtrsim 2kG$, consistent with the conclusion drawn from the dependence of U_0 vs H.

In conclusion, we have demonstrated that resistive tails in a 2D Nb single-crystal film under applied fields can be

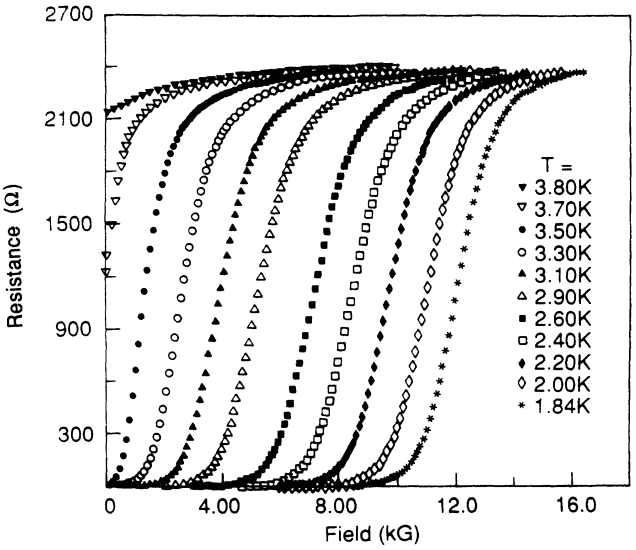

FIG. 17. R vs H at various temperatures.

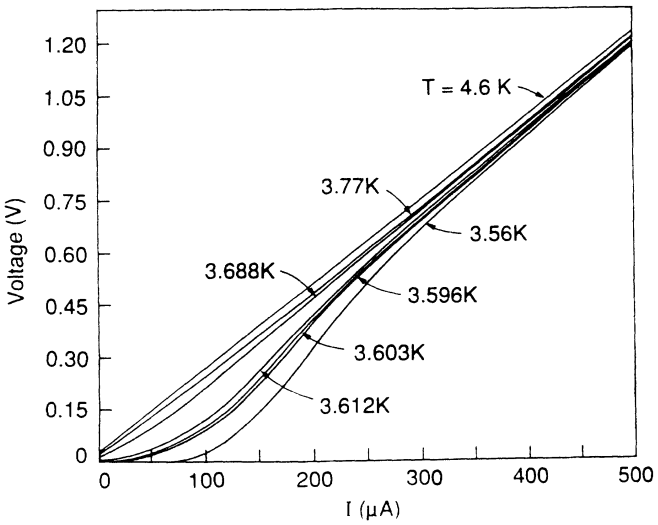

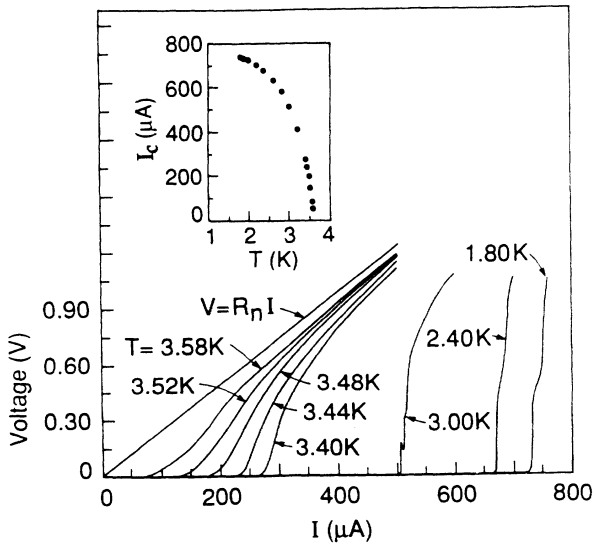

FIG. 16. Voltage vs current in zero field for various temperatures (a) near T_c and (b) below T_c. The inset in (b) shows the temperature dependence of I_c, defined as the current at which dissipation is first measured.

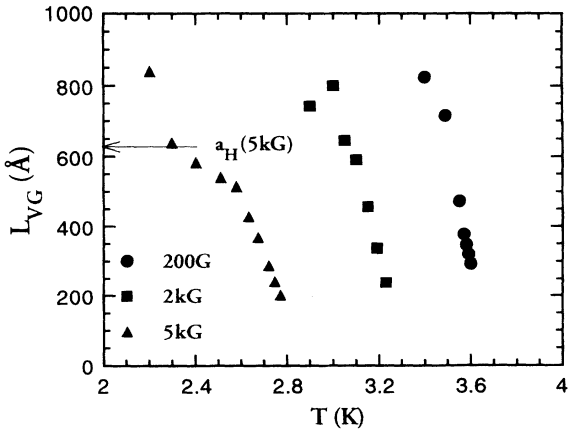

FIG. 18. Vortex-hopping distance vs temperature at $H=200$ G, 2 kG, and 5 kG. a_h for 5 kG is also indicated in the figure. a_h for 2 kG is 1000 Å and for 200 G is 3160 Å. Both integrals are larger than L_{VG} shown here.

explained within the model of flux creep. A reasonable understanding of the pinning source in our system has been obtained. Comparisons with the Bi-Sr-Ca-Cu-O superconductors show strong similarities, indicating the importance of two dimensionality on flux motion in cuprate superconductors.

VI. DISAPPEARANCE OF SUPERCONDUCTIVITY

In the absence of superconductivity, the resistance of a 2D metal increases logarithmically as temperature decreases, a result of weak localization and electron-electron interaction.[33] Weak-localization theory is a noninteracting picture which says that, in the presence of disorder, the probability of coherent backscattering is enhanced. This enhancement is sensitive to time-reversal symmetry-breaking perturbations, such as external magnetic fields. Electron-electron interaction theory predicts resistance with the same temperature dependence and similar coefficients as in the localization theory. However, the contribution from interaction theory to the dc conductivity is much less sensitive to magnetic fields than that from the localization theory. To separate the two effects, one must perform different experiments on the same sample: R vs T together with magnetoresistance or Hall measurements. Including both contributions, the total correction to the resistance has the form

$$\frac{\Delta R}{R_0} = -A\left[\frac{e^2 R_0}{2\pi^2\hbar}\right]\ln\left[\frac{T\tau_\phi}{\hbar}\right], \tag{29}$$

where all resistances are in sheet quantity, A is a numerical factor of order of unity, and τ_ϕ is the shortest time scale in which the electron wave function retains its coherence. In the absence of magnetic fields,

$$\frac{1}{\tau_\phi} = \frac{1}{\tau_{e\text{-ph}}} + \frac{1}{\tau_{e\text{-}e}}, \tag{30}$$

where $\tau_{e\text{-ph}}$ and $\tau_{e\text{-}e}$ are the electron-phonon and electron-electron scattering time. At high fields, τ_ϕ will be replaced by the phase-breaking time (t_H) associated with H (i.e., $t_H \ll \tau_\phi$), t_H being defined as

$$t_H \simeq \frac{\Phi_0}{HD} \simeq \frac{\hbar c}{2eDH}, \tag{31}$$

where D is the diffusion constant. In addition, the spin-orbit scattering suppresses the localization and introduces complications in theoretical calculations.

Figure 19 shows R vs T for the 2D Nb film in $H=2$ and 8 T; the inset shows an enlarged section for the R-vs-T curve for $H=2$ T. For $H=8$ T, the resistance increases logarithmically as temperature decreases, as predicted for 2D metals. The data can be fitted with

$$R(T) = R_0 - r\ln\left[\frac{T}{T_0}\right], \tag{32}$$

with $R_0=121.3\ \Omega/\square$, $r=0.26\ \Omega/\square$, and $T_0=20.2$ K. (See Fig. 20.) Equation (32) is of the same form as the theoretical prediction Eq. (29). Equating r/R_0 to $Ae^2R_0/2\pi^2\hbar$, we obtain $A\approx 1.43$, in agrreement with

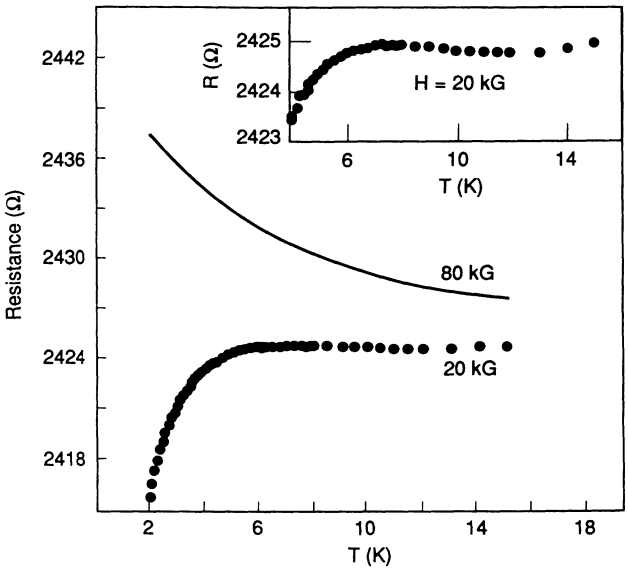

FIG. 19. Resistance vs temperature for $H=2$ and 8 T.

theory. Moreover, $T_0=20.2$ K corresponds to a phase-breaking time of $\tau_\phi=\hbar/kT_0=4\times10^{-13}$ sec, which is comparable to the estimated value of $t_H=2.8\times10^{-13}$ sec for $H=8$ T using Eq. (31). This value is much smaller than the result obtained from zero-field fluctuation-conductivity measurements (see Sec. III), implying that the magnetic field is the dominant phase-breaking mechanism. Hence, after superconductivity is quenched by an external magnetic field, our sample exhibits a behavior of 2D metals in accordance with theory. One might ask why an 8-T external field does not destroy the effect of weak localization. While it is true that the maximally crossed diagrams are sensitive to magnetic fields and the contribution due to the localization effect is suppressed at moderate fields (~kG), the Cooper channel in the interaction effect is not affected until a higher field:

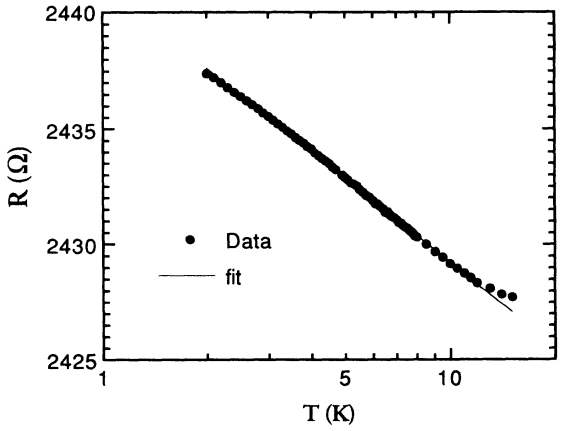

FIG. 20. R vs T (logarithmic) for $H=8$ T. The symbols are the data and the line is the fit.

$$H_{\rm int}=\frac{\pi cT}{2eD}$$
$$\simeq 9\ \text{T at } T=10\ \text{K}.$$

Furthermore, the diffusion channel in the interaction theory, which also gives $\Delta R \propto \ln T$, is not sensitive to magnetic fields.[33] Therefore, it is not surprising that a $\ln T$ dependence of resistance exists at $H=8$ T.

For $H=2$ T, a small amount of superconducting fluctuation is still seen at low temperature, but the increase in resistance due to the electron-electron interaction is also evident. These two competing effects cause the R-vs-T curve to exhibit a maximum. (See Fig. 19, inset.)

VII. SUMMARY

In this paper we have studied various transport properties of a 2D single-crystal Nb film with $d=20$ Å, $R_\square=122\ \Omega/\square$, and $T_c=3.725$ K. In perpendicular fields the resistive tails are caused by thermally activated flux motion, which can be explained by the Anderson-Kim theory extended to 2D with a temperature-dependent activation energy. Zero-field fluctuation conductivity includes both the Aslamov-Larkin and Maki-Thompson contributions, indicating that the film is clean. The pair-breaking parameter δ obtained this way is in agreement with experimental results in the literature. In addition, δ diverges as T_c is approached from above; this phenomenon has been observed before in other thin-film materials with small $R_\square$. In a shielded Dewar, resistance displays a temperature dependence characteristic of that of the Kosterlitz-Thouless transition. The Kosterlitz-Thouless transition temperature $T_{\rm KT}$ was determined using two methods, yielding $T_{\rm KT}=3.565-3.60$ K. This signature of the Kosteriilz-Thouless transition disappears in small perpendicular applied fields ($\gtrsim 10$ G). In a field of 8 T, no sign of superconductivity was seen for temperature above 1.6 K. In this case a $\ln T$ dependence of resistance, characteristic of a 2D metal, was observed. Contrary to perpendicular fields, parallel fields do not affect the superconducting transition below 5 kG; that is, the superconducting transition is neither broadened nor shifted down in temperature for $H_\parallel \lesssim 5$ kG. The effect of strong pinning seems to determine the results of I-V measurements. No evidence the classical flux-flow behavior $R \propto H$ was observed.

Research of clean 2D superconductors has so far been limited because of the difficulty in sample preparation. However, many interesting phenomena which are different from the dirty case have not yet been understood. More theoretical work is also needed. In particular, the pair-breaking model assumes a diffusive behavior for electrons. One might expect this theory to fail when the mean free path is limited by the thickness.

ACKNOWLEDGMENTS

We would like to thank Y. Xu for his help in sample preparation, Mark Lee and S. Ryu for their help during the measurements, and S. Doniach and G. Deutscher for many useful discussions. J. W. P. Hsu would like to acknowledge the support of the Hertz Foundation. This project is supported by NSF.

*Present address: AT&T Bell Labs, 600 Mountain Avenue, Murray Hill, NJ 07974.

[1]J. Halbritter, Appl. Phys. A **43**, 1 (1987).
[2]P. Santhanam, S. Wind, and D. E. Prober, Phys. Rev. B **35**, 3188 (1987), and references cited therein.
[3]P. M. Horn and R. D. Parks, Phys. Rev. B **4**, 2178 (1971).
[4]J. M. Graybeal and M. R. Beasley, Phys. Rev. Lett. **56**, 173 (1986).
[5]Sung I. Park, Ph.D dissertation, Stanford University, 1986.
[6]J. W. P. Hsu and A. Kapitulnik, Appl. Phys. Lett. **17**, 1061 (1990).
[7]Sung I. Park *et al.*, J. Mater. Res. **2**, 446 (1987).
[8]W. J. Skocpol and M. Tinkham, Rep. Prog. Phys. **38**, 1049 (1975).
[9]B. I. Halperin and David R. Nelson, J. Low Temp. Phys. **36**, 599 (1979).
[10]V. G. Kogan, Phys. Rev. B **32**, 139 (1985); **34**, 3499 (1986); Vladimir G. Kogan and Norio Nakawa, *ibid.* **35**, 1700 (1987).
[11]M. Tinkham, *Introduction to Superconductivity* (Kriger, Malabar, FL, 1985).
[12]*Introduction to Superconductivity* (Ref. 11), pp. 264–268.
[13]H. R. Kerchner, D. K. Christen, and S. T. Sekula, Phys. Rev. **24**, 1200 (1981).
[14]L. G. Aslamazov and A. I. Larkin, Phys. Lett. **26A**, 238 (1968).
[15]K. Maki, Prog. Theor. Phys. **39**, 897 (1968).
[16]R. S. Thompson, Phys. Rev. B **1**, 327 (1970).
[17]R. E. Glover III, Physica **55**, 3 (1971).
[18]See, e.g., Koji Kajumura and Nobuo Mikoshiba, J. Low Temp. Phys. **4**, 331 (1971).
[19]J. E. Crow, A. K. Bhatnager, and T. Mihalisn, Phys. Rev. Lett. **28**, 25 (1972).
[20]Bruce R. Patton, Phys. Rev. Lett. **27**, 1273 (1971).
[21]R. A. Craven, G. A. Thomas, and R. D. Parks, Phys. Rev. B **7**, 147 (1973).
[22]James M. Gordon, C. J. Lobb, and M. Tinkham, Phys. Rev. B **29**, 5232 (1984).
[23]John M. Graybeal, Ph.D. dissertation, Stanford University, 1985.
[24]A. F. Hebard and M. A. Paalanen, Phys. Rev. B **30**, 4063 (1984).
[25]E. Abrahams *et al.*, Phys. Rev. B **24**, 6783 (1981).
[26]M. E. Gershenzon, V. N. Gubankov, and Yu. E. Zhuravlev, Zh. Eksp. Teor. Fiz. **85**, 287 (1983) [Sov. Phys. JETP **58**, 167 (1983)].
[27]Bruce J. Dalrymple *et al.*, Phys. Rev. B **33**, 7514 (1986).
[28]T. Kawagut and Y. Shibuya, Phys. Lett. **45A**, 395 (1973).
[29]J. Apple, Phys. Rev. Lett. **21**, 1164 (1968).
[30]E. L. Wolf, *Principles of Electron Tunneling Spectroscopy* (Oxford University Press, London, 1985), p. 523.
[31]N. W. Ashcroft and N. D. Mermin, *Solid State Physics* (Saunders College, Philadelphia, 1976), p. 38.
[32]M. Hikita, Y. Tajima, and T. Tamamura, in *Anderson Localization*, edited by T. Ando and H. Fukuyama (Springer-Verlag,

Berlin, 1988), p. 207.
[33]B. L. Altschuler and A. G. Aronov, in *Electron-Electron Interactions in Disordred Systems,* edited by A. L. Efros and M. Pollak (North-Holland, Amsterdam, 1985), p. 1
[34]C. Van Haesendonck, M. Gijs, and Y. Bruynseraede, in *Localization, Interaction, and Transport Phenomena,* edited by B. Kramer, G. Bergmann, and Y. Bruynseraede (Springer-Verlag, Berlin, 1985), p. 221.
[35]Koya Aoi, R. Meservey, and P. M. Tedrow, Phys. Rev. B **9**, 875 (1974).
[36]J. M. Kosterlitz and D. J. Thouless, J. Phys. C **6**, 1181 (1973).
[37]J. Pearl, in *Low Temperature Physics—LT9,* edited by J. G. Daunt, D.O. Edwards, F. J. Milford, and M. Yagub (Plenum, New York, 1965), p. 566.
[38]M. R. Beasley, J. E. Mooij, and T. P. Orlando, Phys. Rev. Lett. **42**, 1165 (1979).
[39]P. Minnhagen, Phys. Rev. B **27**, 2807 (1983); **28**, 2463 (1983); **29**, 1440 (1984).
[40]J. C. Garland and Hu Jong Lee, Phys. Rev. B **36**, 3638 (1987).
[41]J. E. Mooij, in *Percolation, Localization, and Superconductivity,* edited by A. M. Goldman and S. A. Wolf (Plenum, New York, 1984), p. 325.
[42]S. Doniach and B. A. Huberman, Phys. Rev. Lett. **42**, 1169 (1979).
[43]A. F. Hebard and A. T. Fiory, Phys. Rev. Lett. **50**, 1603 (1983).
[44]A. F. Hebard and A. T. Fiory, Phys. Rev. Lett. **44**, 291 (1980).
[45]B. Oh *et al.*, Phys. Rev. B **37**, 7861 (1988).
[46]T. T. M. Palstra, B. Batlogg, L. F. Schneemeyer, and J. V. Waszczak, Phys. Rev. Lett. **61**, 1662 (1988).
[47]P. W. Anderson and Y. B. Kim, Rev. Mod. Phys. **36**, 39 (1964).
[48]P. W. Anderson, Phys. Rev. Lett. **9**, 309 (1962).
[49]B. A. Huberman and S. Doniach, Phys. Rev. Lett. **43**, 950 (1979).
[50]Daniel S. Fisher, Phys. Rev. B **22**, 1190 (1980).
[51]H. A. Kramers, Physica **7**, 284 (1940).
[52]Y. Yeshurun and A. P. Malozemoff, Phys. Rev. Lett. **60**, 2202 (1988).
[53]M. Tinkham, Phys. Rev. Lett. **61**, 1658 (1988).
[54]S. Doniach, in *Temperature Superconductivity Proceedings,* edited by K. S. Bedell, D. Coffey, D. E. Meltzer, D. Pines, and J. R. Schrieffer (Addison-Wesley, Redwood City, CA, 1990), p. 406.
[55]J. Bardeen and M. J. Stephen, Phys. Rev. **140**, A1197 (1965).
[56]S. Martin, Phys. Rev. B **43**, 6523 (1991); M. Inui, P. Littlewood, and S. Coopersmith, Phys. Rev. Lett. **44**, 3333 (1989).
[57]C. W. Hagen and R. Griessen, Phys. Rev. Lett. **62**, 2857 (1989).
[58]R. C. Barrett and C. F. Quate, J. Vac. Sci. Technol. A **8**, 400 (1990).
[59]Jonathan Zn Hong Sun, Ph.D. dissertation, Stanford University, 1989.
[60]R. H. Koch *et al.*, Phys. Rev. Lett. **63**, 1151 (1989).
[61]D. S. Fisher, M. P. A. Fisher, and D. A. Huse, Phys. Rev. B **43**, 130 (1991).

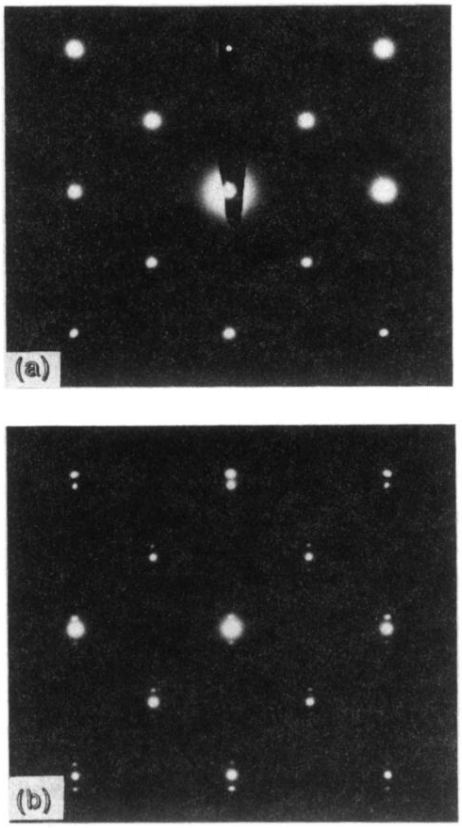

FIG. 1. Typical TEM diffraction patterns of ultrathin Nb described in the text: (a) sample with ion-beam-cleaned substrate (A2) and (b) sample with uncleaned substrate (A3).